Soc. **1988**, *110*, 4494. For the systems studied, the Smoluchowski equation worked well with *measured* diffusion constants but not with those estimated by the Stokes-Einstein equation.

Registry No. Bromine, 7726-95-6; tribromide ion, 14522-80-6; 2,4,6-tribromophenol, 118-79-6; 2,4,6-tribromophenol anion, 65800-38-6; phenol, 108-95-2; phenoxide, 3229-70-7; 2,4-dimethylphenol, 105-67-9; 2,6-dimethylphenol, 576-26-1; 2-nitrophenol, 88-75-5; 2-nitrophenoxide, 16554-53-3; 3-nitrophenol, 554-84-7; 3-nitrophenoxide, 16554-54-4; 4-cyanophenol, 767-00-0; 4-cyanophenoxide, 14609-76-8; 4-nitrophenol, 100-02-7; 4-nitrophenoxide, 14609-74-6; 2-pyrimidone, 557-01-7; 2-pyrimidone anion, 33631-11-7; 4-pyrimidone, 4562-27-0; 4-pyrimidone anion, 3273-54-9; 4-bromophenol, 106-41-2.

Supplementary Material Available: Tables of second-order rate constants for the bromination of phenols and pyrimidones as a function of various concentrations (Tables S1-S5) (5 pages). Ordering information is given on any current masthead page.

Matrix-Isolation Decay Kinetics of Triplet Cyclobutanediyls. Observation of Both Arrhenius Behavior and Heavy-Atom Tunneling in C-C Bond-Forming Reactions

Michael B. Sponsler,[1a] Rakesh Jain, Frank D. Coms,[1b] and Dennis A. Dougherty*

Contribution No. 7820 from the Arnold and Mabel Beckman Laboratory of Chemical Synthesis, 164-30, California Institute of Technology, Pasadena, California 91125. Received July 28, 1988

Abstract: The ring-closure reactions of a variety of triplet 1,3-cyclobutanediyls (**1**) have been observed by EPR spectroscopy under matrix-isolation conditions. It is shown that matrix-site effects can be very well modeled by a Gaussian distribution of activation energies with a standard deviation of ca. 0.5 kcal/mol. Several new techniques have been developed to model such dispersive kinetics. Structures **1** with delocalizing substituents (vinyl, phenyl) show conventional Arrhenius behavior, with log A = 6-8 and E_a = 1-2 kcal/mol. Fully localized cyclobutanediyls ring close via quantum mechanical tunneling. A model emphasizing the differing well depths of the singlet biradicals is developed to rationalize these contrasting behaviors.

The direct spectroscopic characterization of reactive intermediates has been a major focus of modern mechanistic chemistry. Through such studies, one can determine whether the thermodynamic and kinetic properties of a reactive intermediate are consistent with those ascribed inferentially on the basis of product distributions, stereochemical labeling, and other classical techniques. Laser-flash photolysis and related fast spectroscopy techniques have often been successfully applied to such studies. However, there are many types of reactive intermediates that do not have a well-characterized chromophore and an unambiguous, efficient mode of generation. Both of these are necessary for the laser-flash methods, which generally have relatively low spectroscopic resolution. The matrix-isolation technique is an alternative approach for providing high-resolution spectroscopic data on reactive structures. However, for kinetic studies, it has been less broadly successful, at least in part because of "matrix-site effects". In a nonfluid medium at cryogenic temperatures, different molecules in a sample experience different microenvironments. These matrix perturbations generally lead to complex (dispersive) kinetic behavior, because, in principle, each site has its own intrinsic decay rate.

We have recently reported the synthesis and EPR spectroscopy of several 1,3-disubstituted 1,3-cyclobutanediyls (**1**), the first series of directly observed, localized 1,3-biradicals.[2] We now describe the matrix-isolation decay behavior of several members of the series as monitored by EPR spectroscopy. For the purpose of discussion, it is convenient to divide the cyclobutanediyls into two classes, those with delocalizing substituents and those without. We shall refer to the first group (**1**-Vin, **1**-EV, **1**-Ph) as stabilized and the second (**1**-Me, **1**-Et) as fully localized.

We have made a considerable effort to address the matrix-site problem and have developed several new techniques and analytical approaches. This report contains much description of methodology and of detailed efforts to accurately quantify the results obtained. In the course of such discussions, one can lose sight of the more far-reaching, general findings of the work. We therefore summarize, at the outset, the important qualitative conclusions we have reached concerning the decay of triplet cyclobutanediyls.

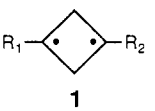

1

1-H	$R_1 = R_2 = H$
1-Me	$R_1 = R_2 = CH_3$
1-Et	$R_1 = R_2 = CH_2CH_3$
1-Vin	$R_1 = R_2 = CH{=}CH_2$
1-Ph	$R_1 = R_2 = Ph$
1-EV	$R_1 = CH_2CH_3$ $R_2 = CH{=}CH_2$

2

First, by using a novel technique termed "distribution slicing", we have been able to demonstrate unambiguously for **1**-Vin, **1**-EV, and **1**-Ph that there *is* a matrix-site effect. That is, photolysis of diazabicyclohexenes (**2**) in frozen-solvent matrices produces cyclobutanediyls (**1**) in a range of matrix sites with differing decay behaviors. Importantly, the distribution-slicing method clearly shows that there is a distribution of E_a values among the matrix sites. This rules out one type of analysis which assumes a distribution of Arrhenius preexponential terms (A), with a constant E_a. More detailed analysis strongly indicates that the rate distribution is primarily a consequence of a distribution over E_a and is relatively insensitive to any variation in A. In addition, the distribution-slicing method provides qualitative information on the width and the shape of the rate distribution. We find that a Gaussian distribution of E_a values is an excellent model for these systems.

Second, by combining distribution slicing with a new method of directly fitting decay traces, we have been able to obtain most probable decay rates over a sizable temperature range for **1**-Vin, **1**-EV, and **1**-Ph. These rates clearly follow the Arrhenius law. These structures are the first localized 1,3-biradicals for which

(1) (a) NSF Predoctoral Fellow, 1982-1985. (b) JPL-CSMT Fellow, 1987-1988.

(2) Jain, R.; Sponsler, M. B.; Coms, F. D.; Dougherty, D. A. *J. Am. Chem. Soc.* **1988**, *110*, 1356-1366. Jain, R.; Snyder, G. J.; Dougherty, D. A. *J. Am. Chem. Soc.* **1984**, *106*, 7294-7295.

0002-7863/89/1511-2240$01.50/0 © 1989 American Chemical Society

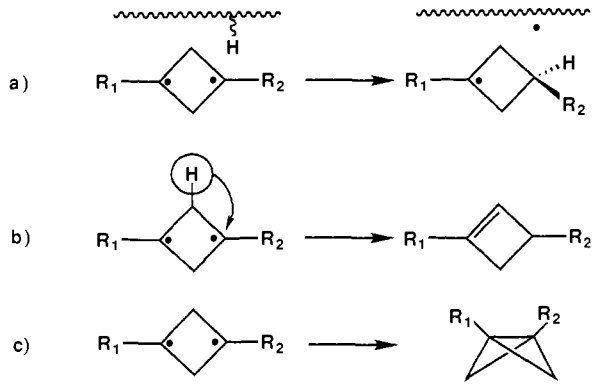

Figure 1. Possible decay pathways for cyclobutanediyls: (a) abstraction of H atom from solvent, (b) intramolecular 1,2-H shift, and (c) intramolecular coupling of two radical centers.

such behavior has been observed.

In striking contrast to these stabilized biradicals, the fully localized structures **1**-Me and **1**-Et show a fundamentally different decay pattern. No scheme assuming Arrhenius behavior and any type of distribution of sites can adequately model the decay kinetics for these structures. Essentially, the decay rates are independent of temperature at low temperatures. Closs has previously reported[3] similar behavior for another localized 1,3-biradical, cyclopentanediyl (**3**). Studies on **3** using our distribution model fully support Closs' original analysis. Quantum mechanical tunneling appears to be involved in the decay of these molecules.

3

Most importantly, **1**-Et, **1**-EV, and **1**-Vin are almost identical in terms of their steric interactions with the matrix. Yet, they show fundamentally different decay behaviors. This proves that *matrix-restraining forces are not exclusively responsible for the decay patterns we see.* The electronic structure of the biradical is a determining factor. Thus, the approaches outlined herein hold the potential for establishing the effects of structural changes on the fundamental chemistry of simple biradicals.

General Considerations

The Decay Products. Prior to describing our analysis of the cyclobutanediyl decay kinetics, it is important to establish the nature of the decay process. We have considered three possibilities, shown in Figure 1. Radical hydrogen abstraction from the solvent matrix, probably the most commonly studied reaction at cryogenic temperatures,[4-6] was ruled out by several lines of evidence. First, the observed decay of the cyclobutanediyls is much faster than any known abstraction process. Hydrogen abstraction by radicals and carbenes is most often studied at 77 K or higher, whereas all our studies on cyclobutanediyls have been carried out below 65 K. Second, decay of the triplet signals corresponding to **1** is *not* accompanied by growth of any doublet signals, which would be expected from the resulting cyclobutyl and solvent radicals. Finally, comparison of decay rates in protio vs deuterio solvents (**1**-Vin in pentane vs pentane-d_{12} and **1**-Me in acetone vs acetone-d_6) shows no difference in rates. Such an abstraction reaction should show a large kinetic isotope effect at such low temperatures, especially if tunneling is involved.[6]

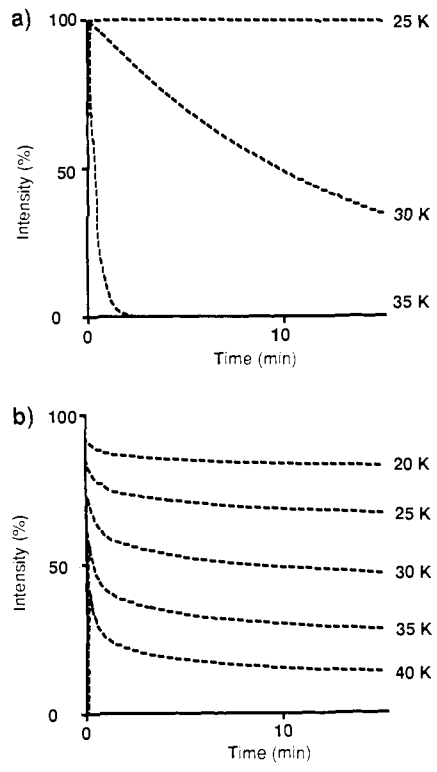

Figure 2. Simulated decay of an Arrhenius process (log A = 8.0) with (a) $E_a°$ = 1.5 kcal/mol, and (b) Gaussian distribution over energy of activation, E_a = 1.5 kcal/mol and standard deviation (σ) = 0.5 kcal/mol. The rates (s^{-1}) involved (single rates in (a), most probable rates in (b)) are the following: 20 K, 4.0×10^{-9}; 25 K, 7.7×10^{-6}; 30 K, 1.2×10^{-3}; 35 K, 4.3×10^{-2} and; 40 K, 6.4×10^{-1}. Photolysis time is 5 s in all cases.

The other two possible decay processes, closure to give bicyclobutanes and 1,2-hydrogen shift to give cyclobutenes (Figure 1), will be considered together. Compelling evidence comes from product analysis of EPR samples. High-field NMR analysis of a sample of **2**-Vin (in deuteriochloroform) which had been photolyzed many times in EPR experiments showed conversion to the bicyclobutane closure product, with no signs of a cyclobutene.[7] A similar result was obtained for a sample of **2**-Me in acetone-d_6, with both NMR and GC analyses.[8] In addition, in all of our extensive studies of the solution-phase thermal chemistry and photochemistry of various diazabicyclohexenes (**2**) we have seen no evidence of cyclobutene products.[2,9] We feel this rules out cyclobutene formation as the decay path for cyclobutanediyls.

In support of this, we note that Fisher and Michl[10] have recently observed both processes in the same biradical, a naphthoquinodimethane (**4**), under separate conditions. The hydrogen-shift

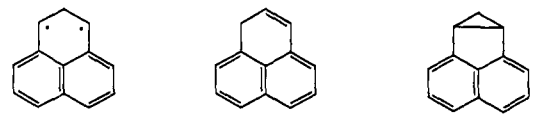

4 **5** **6**

reaction, producing **5**, occurred in a purely exponential fashion, and a conventional analysis produced activation parameters. In contrast, the closure process, giving **6** was characterized by nonexponential kinetics attributed to a matrix effect resulting from a larger geometrical change. Cyclobutanediyls **1** display *strongly* nonexponential decay. This behavior is more consistent with the closure pathway, given Michl's work.

(3) Buchwalter, S. L.; Closs, G. L. *J. Am. Chem. Soc.* **1975**, *97*, 3857-3858. Buchwalter, S. L.; Closs, G. L. *J. Am. Chem. Soc.* **1979**, *101*, 4688-4694.

(4) French, W. G.; Willard, J. E. *J. Phys. Chem.* **1968**, *72*, 4604-4608. Williams, F.; Sprague, E. D. *Acc. Chem. Res.* **1982**, *15*, 408-415.

(5) Doba, T.; Ingold, K. U.; Siebrand, W.; Wildman, T. A. *J. Phys. Chem.* **1984**, *88*, 3165-3167. Doba, T.; Ingold, K. U.; Siebrand, W. *Chem. Phys. Lett.* **1984**, *103*, 339-342.

(6) See, for example, Platz, M. S.; Senthilnathan, V. P.; Wright, B. B.; McCurdy, C. W., Jr. *J. Am. Chem. Soc.* **1982**, *104*, 6494-6501, and references therein.

(7) Sponsler, M. B. Ph.D. Thesis, California Institute of Technology, 1987. This work also contains source listings for all relevant computer programs and more detailed discussions of the various kinetics-modeling schemes.

(8) Jain, R. Ph.D. Thesis, California Institute of Technology, 1987.

(9) Chang, M. H.; Jain, R.; Dougherty, D. A. *J. Am. Chem. Soc.* **1984**, *106*, 4211-4217. Chang, M. H.; Dougherty, D. A. *J. Am. Chem. Soc.* **1982**, *104*, 2333-2334.

(10) Fisher, J. J.; Michl, J. *J. Am. Chem. Soc.* **1987**, *109*, 583-584.

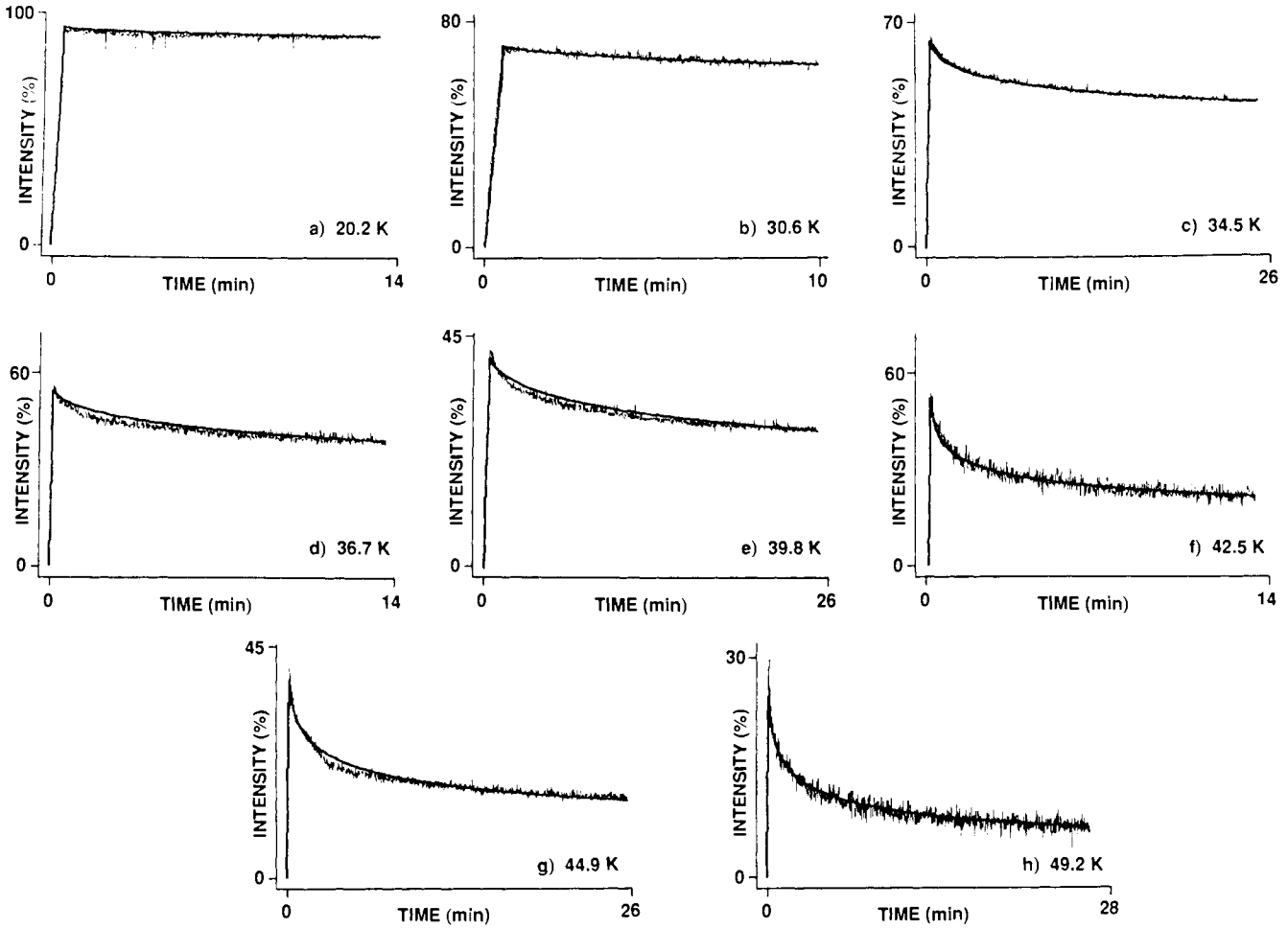

Figure 3. Experimental and calculated decay traces for **1**-Vin in MTHF analyzed by using the σ_{DS} procedure (see the text). The fits were obtained with σ_{DS} = 0.523 kcal/mol. Optimization of photolysis heating gave the following values: (a) 1.4 K, (b) 3.7 K, (c) 2.2 K, (d) 6.5 K, (e) 5.5 K, (f) 1.5 K, (g) 3.6 K, and (h) 4.0 K.

Thus, the process we are observing represents perhaps the most fundamental of organic reactions—the direct coupling of two radical centers to make a new C–C bond. Concomitant with bond formation, intersystem crossing must occur, as this is the spin-forbidden, triplet→singlet incarnation of radical coupling.

Anticipated Decay Patterns. Before discussing our results, consideration of typical kinetic behavior at cryogenic temperatures, with and without a matrix effect, would be helpful. Presuming, for the moment, that the reaction under study shows exponential and Arrhenius (nontunneling) behavior, the temperature range in which the reaction would occur on a convenient time scale would be quite small. For example, Figure 2a shows predicted decay traces for a process with log A = 8.0 and E_a = 1.5 kcal/mol at 25, 30, and 35 K. Over a range of 10 K, the reaction rate varies by nearly 4 orders of magnitude. This illustrates the much greater sensitivity of reaction rates to small temperature changes at very low temperatures. Such a reaction would present severe obstacles to anyone attempting to accurately measure its activation parameters, since temperatures would have to be maintained with high precision and measured with high accuracy, both difficult tasks below 77 K.

Suppose next that the reaction has a distribution of activation energies but still displays Arrhenius behavior. Simulated decays (obtained as described below) are shown in Figure 2b, assuming the same activation parameters as in Figure 2a and a Gaussian E_a distribution with a standard deviation (σ) of 0.5 kcal/mol. The temperature range over which decay is observable is much larger, even though the most probable rates are the same at a given temperature. Note that the signal intensities are never 100% due to decay during the photolysis interval (see below). This situation represents a trade-off for the experimentalist in search of activation parameters; in return for the expanded temperature range, the complexity of the problem has increased enormously. As shown in Figure 3, our experimental data are consistent with such a distribution over E_a.

An important point illustrated by Figures 2b and 3 is the fact that all the decay traces in a composite first-order system are similar in shape, differing mainly in intensity. This observation can be explained by dividing the distribution into three components for any given decay trace, as done for the 20 and 40 K traces in Figure 4. The three components are (1) the "fast sites", which have rate constants too high to allow observation at the given temperature, (2) the "slow sites", which are completely stable on the time scale of the experiment, and (3) the "intermediate sites" (shaded in Figure 4), which account for all of the observed decay. The intermediate sites for the two temperatures have the same range of rate constants, which explains the similarity in the shape of the decay traces. The important feature in determining shape, then, is simply the ratio of intermediate sites to slow sites.

Methodologies for Modeling Dispersive Kinetics

In this section we will describe the development and implementation of the various modeling techniques we have used to analyze the decay behavior of the cyclobutanediyls. For the sake of illustration we will describe in detail our studies of **1**-Vin in 2-methyltetrahydrofuran (MTHF). This is the system we have investigated most intensively, and it is well-suited to the modeling procedures. The Results section will describe the applications of these techniques to several different cyclobutanediyls in several different solvents.

In all experiments, EPR samples were prepared by taking a degassed solution of the appropriate diazene (**2**) and quickly

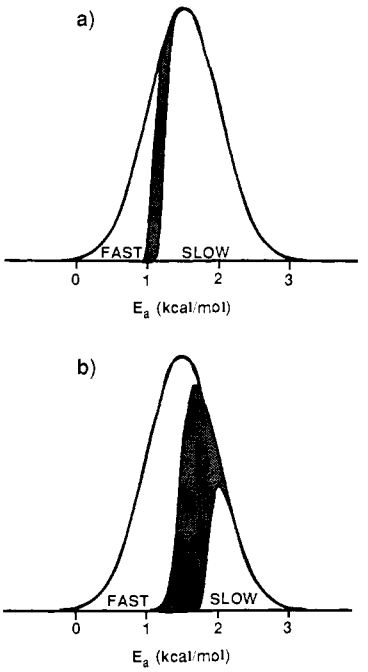

Figure 4. Division of a distribution into fast, intermediate (shaded), and slow sites at (a) 20 K and (b) 40 K. The observed decay corresponds to the shaded portions of the distribution.

immersing it in liquid nitrogen to form the glassy or polycrystalline matrix. Thus, regardless of the conditions of a particular kinetics experiment, we assume that for a given solvent all samples of a given diazene have the same initial distribution of diazene sites.

Distribution Slicing.[7] In a matrix-isolation experiment, the rigid medium suppresses bimolecular chemistry (except reaction with the matrix material), so only unimolecular decay processes are viable. One would expect simple, exponential decays, but as discussed above, this is not generally the case. Our initial efforts at evaluating cyclobutanediyl reactivity involved photolysis of the precursor diazenes for short times at various temperatures to generate adequate EPR signals and then monitoring the decay of the EPR signals over time. As described in detail below, these decays were highly nonexponential. Early attempts at decay simulation achieved a limited success. These preliminary simulations, however, did clearly suggest that we were observing a matrix-site effect involving a distribution of E_a values. We felt it was necessary, though, to obtain independent evidence for such a distribution over E_a. We thus developed the distribution-slicing method, which not only confirmed the existence of the site distribution but also directly provided information on the nature of the distribution. Such information was crucial to the success of our decay-simulation efforts.

Conceptually and experimentally, the distribution-slicing method is relatively simple. A signal that represents an intact E_a distribution is generated by photolysis at a temperature low enough to ensure that no decay occurs. For **1**-Vin, **1**-EV, and **1**-Ph, 3.8 K is sufficient. Then, by warming the matrix to successively higher temperatures, fast sites are in effect sliced off the distribution in layers (see Figure 5). By recooling to 3.8 K in-between warming cycles and measuring the signal intensity, the size of each "slice" (relative to the intact distribution) can be obtained. Reconstruction of the distribution from the constituent slices (Figure 5f) then produces a crude image of the distribution.

As shown in Figure 6, even the boundary line of a slice spans a significant range in E_a, which defines a "resolution" of the method. Our objective in the experiment is to assign a single E_a value to the slice so that the overall E_a distribution may be reconstructed directly. Starting with the Arrhenius equation (eq 1), the rate, k, is assigned to the sites which experience 50% decay

$$E_a = -RT \ln (k/A) \quad (1)$$

during the warming interval (see Figure 6). In other words, the

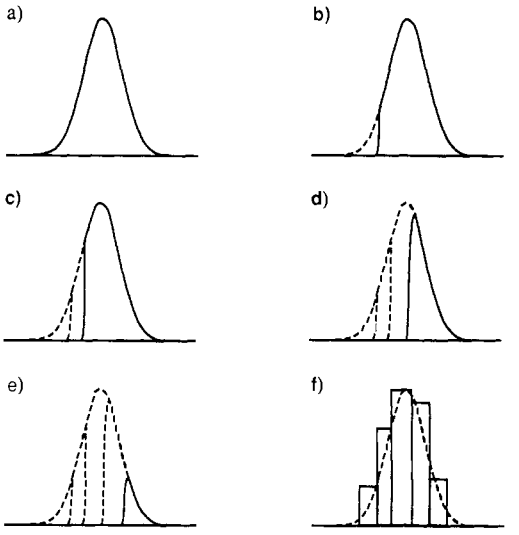

Figure 5. A distribution-slicing experiment, on an E_a scale: (a) intact distribution; (b–e) evolution of the distribution during warmings to successively higher temperatures [the area bounded by the solid line represents the sites that remain (and thus the signal intensity) after warming]; (f) reconstruction of the distribution.

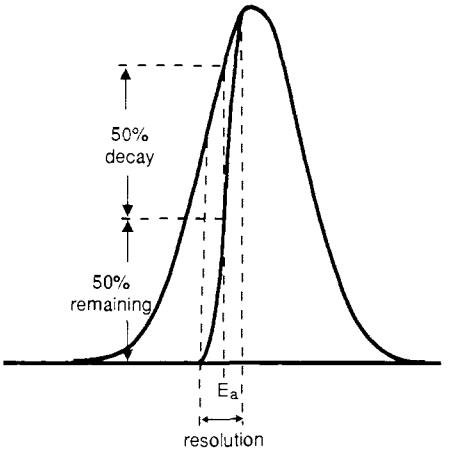

Figure 6. Assignment of a representative E_a to a given slice.

warming interval corresponds to exactly 1 half-life for these sites. Therefore

$$\text{warming interval} = t = (\ln 2)/k \quad (2)$$

Substitution into eq 1 gives

$$E_a = -RT \ln ((\ln 2)/At) \quad (3)$$

The value of T is known from the experiment, and we must assume a value for A (see below). Thus, E_a is easily calculated.

Reconstruction of the distribution from the slicing experiment, as shown in Figure 5f, involves conversion of the intensity data into areas under the distribution and as such constitutes a form of numerical differentiation. This type of process always results in magnification of errors, and for this reason it is perhaps preferable to present the results in the integrated (intensity vs E_a) form. Distribution-shape information is still available in this format, as shown in Figure 7 for Gaussian, box, and right-triangle distributions.

As an example, data from a distribution-slicing experiment for **1**-Vin in MTHF are listed in Table I. The raw data for each cycle include the temperature to which the matrix was warmed, the warming interval, and the intensity recorded upon recooling. In order to plot the data, the temperature and time values were first converted to E_a values with eq 3 and by assuming log A = 8.0. (The choice of log A affects only the E_a values and the width, not the distribution shape.) The plot of intensity vs E_a is shown in Figure 8. This graph, when compared to the curves in Figure

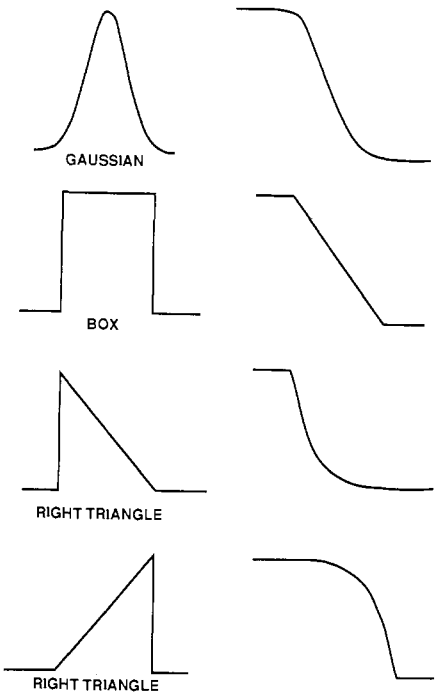

Figure 7. Distribution shapes (probability vs E_a, left) and integrated form of the distributions (intensity vs E_a, right).

Table I. Distribution-Slicing Data for **1**-Vin in MTHF

T, K	t, s	intensity, %	E_a, kcal/mol[a]
3.8	600	100.0	0.19
10.1	98	99.0	0.47
17.8	135	96.8	0.84
17.8	350[b]	95.3	0.87
22.7	270	90.1	1.10
27.2	270	80.1	1.32
34.3	295	53.5	1.67
39.4	190	37.3	1.88
44.5	190	22.4	2.13
50.2	270	9.5	2.43
55.5	270	3.7	2.69

[a] Calculated with equation 3 and log A = 8.0. [b] The experimental time interval for this slice was 215 s. The value shown represents the total time spent at 17.8 K.

7, agrees best with the Gaussian distribution curve. Thus, the distribution shape, which completely eludes decay-fitting procedures (see below), is in effect "photographed" by this comparatively simple procedure.

In addition to providing shape information, this method serves to verify the distribution model itself through simple, qualitative observations. For example, whenever consecutive warming cycles involve the same temperature, the majority of the decay always occurs during the first cycle. Subsequent cycles show very little decay, since the fast sites and many of the sites in the intermediate region have already been depleted. An example of this behavior is shown in Table I for the low-E_a region of the distribution, though similar behavior has been observed throughout the distribution. Furthermore, any subsequent warming cycles to lower temperatures show no decay at all on a reasonable time scale. Note also that the data of Table I are *not* consistent with a distribution over A, with a relatively constant E_a. In such a case decay behavior is essentially invariant to temperature. As far as we are aware, these observations constitute the most direct evidence to date in support of a distribution model.[11]

Our results (such as the example in Figure 8) closely resembled the Gaussian model, and we have used this distribution shape in

(11) Less-direct evidence has been based upon variation of the photolysis intervals and hence the number of fast sites. See ref 12. In addition, "site-clearing" behavior has been seen by Chapman: McMahon, R. J.; Chapman, O. L. *J. Am. Chem. Soc.* **1987**, *109*, 683-692.

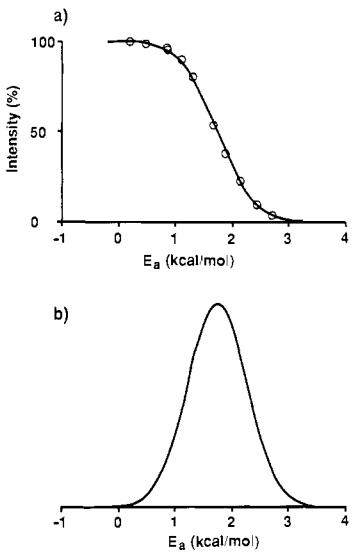

Figure 8. Distribution-slicing results (from DSFIT) for **1**-Vin in MTHF, assuming log A = 8 (Table III): (a) intensity vs E_a fit to a Gaussian and (b) the optimized Gaussian distribution.

all subsequent studies. However, it should be noted that satisfactory fits to the *decay traces* can be obtained with other distributions, including all those of Figure 7.[7] We choose the Gaussian because of the results of Figure 8 and because it seems like a relatively unbiased shape. A computer program to fit the distribution slicing results to the Gaussian model has been developed. The program, called DSFIT, accepts as input from a data file the raw temperature, time, and intensity data (e.g. Table I). The only additional input necessary is log A. The most probable E_a and distribution width (expressed as the standard deviation implied by the Gaussian (σ)) are optimized. The fit obtained for the **1**-Vin example with log A = 8.0 is shown in Figure 8, along with the Gaussian E_a distribution implied by the fit.

The experimental procedure used in distribution slicing has several intrinsic advantages when compared to normal decay kinetics. A significant advantage is that even though the decay may be probed over a large temperature range, all intensity measurements are made at the *same* temperature. This is crucial because in EPR absolute-signal intensity varies considerably with temperature in the 4–65 K range (Curie law). Furthermore, the measurement temperature, usually 3.8 K, is the easiest temperature to attain accurately with a liquid-helium cryostat. As described below, these aspects of distribution slicing are of tremendous value when simulating decay traces.

The method also has several drawbacks. One is that the temperatures must be equilibrated quickly and without overshooting. At such low temperatures, kinetic behavior for a distribution of sites is characterized by a much greater dependence on temperature than on time, so temperature equilibration is a crucial issue. The precise control of liquid-helium cryostats and maintenance of a viable temperature calibration—technical issues that are discussed in detail elsewhere[7]—also complicate the analysis. Further simulations[7] suggest two other limitations of the method. First, the width of the *rate* distribution at any given temperature must be quite substantial, although, as discussed above, this is a common situation at cryogenic temperatures. Second, the total width of the E_a distribution should be large relative to the most probable E_a. In other words, the distribution should extend nearly to zero on the E_a axis. Therefore, the range of reactions for which distribution slicing may be used effectively may be somewhat limited. The present system, though, is well-suited to the technique.

Decay-Trace Fitting. We have also used decay-trace fitting, the usual method of analysis for rate-dispersive kinetics. Extraction of useful rate information from matrix-perturbed kinetic traces has proved to be highly challenging to chemists and physicists, though several methods have been used with success.[5,6,12-14] A

convenient and common assumption in the distribution model and one that we will use is that the rate dispersion arises from a distribution of activation energies (E_a), i.e., that the Arrhenius preexponential term (log A) is a constant. We have already shown that the distribution-slicing data support this assumption. Also, at very low temperatures, the rate is much more sensitive to small variations in E_a than those in log A. For example, at 20 K a change of 0.1 kcal/mol in E_a is equivalent to a change of more than 1 log A unit. Therefore, a distribution that covers a small range over both log A and E_a can usually be approximated by a distribution over E_a alone.

The goal of all methods using a distribution model is to obtain the initial rate-constant distribution or at least its maximum, the most probable rate constant. If we denote the distribution at a given time as $F(k,t)$, then it is well known that the decay-trace kinetic observable $f(t)$ is related to the initial distribution, $F(k,0)$, by the Laplace transform given in eq 4. This relationship implies

$$f(t) = \int_0^\infty F(k,0)e^{-kt}\,dk \tag{4}$$

that the desired distribution can be obtained by Laplace inversion of the kinetics trace, as indicated in eq 5. Unfortunately, nu-

$$F(k,0) = \mathcal{L}^{-1}[f(t)] \tag{5}$$

merical Laplace inversion is an ill-conditioned transformation; i.e. very small changes in $f(t)$ can result in very large changes in $F(k,0)$.

As a consequence of this instability, no general procedure is available for numerically inverting the Laplace transform.[15] However, a number of methods have been developed for specific circumstances,[15,16] and our first approach to decay simulation involved a modification of a published procedure based on numerical quadrature and dynamic programming.[15] When we applied this method to our decay traces, we obtained single-maximum rate distributions which were well-defined by the available points. However, converting the calculated distributions back to the form of decay traces via the forward Laplace transform, a straightforward computation, resulted in poor agreement with the actual decay traces.

A more popular method for obtaining rate distributions involves fitting decay traces to a function whose analytical Laplace inverse is known. Once the function has been chosen, the procedure is quite simple, involving adjustment of one or two parameters to produce the best fit, followed by a simple calculation of the most probable rate. A disadvantage is that the shape of the distribution, which is determined by the function chosen, can be somewhat arbitrary.

In studying the rebinding of carbon monoxide to myoglobin following photodissociation, Austin et al.[13] found that the kinetic data could be fit to the power-law function

$$f(t) = \left(1 + \frac{t}{t_0}\right)^{-n} \tag{6}$$

where n and t_0 are adjustable parameters. This function implies a rate-constant distribution that has its maximum at $k^\circ = n/t_0$. The most probable rate, k°, is thus easily obtained from the best fit to eq 6. However, when we attempted to fit decay data for **1**-Vin to this function, we did not achieve acceptable agreement.

A related procedure involves plotting the decay of the signal $f(t)$ as $\ln f(t)$ vs $t^{1/2}$, rather than the usual plot vs t.[6] Siebrand has shown[5,12] that such an analysis is tantamount to assuming a distribution of the form:

$$F(k,0) = c(4\pi k^3)^{-1/2}e^{-c^2/4k}$$

Again our data was not amenable to a $t^{1/2}$ analysis.

The failure of these and other functions[5,13] to fit our data was probably caused, at least in part, by an inherent assumption of these methods which is invalid in our case. All of the functions describe the decay as starting from $t = 0$ and ignore the perturbation of a finite generation time. This approximation presents no difficulty for a situation in which there are no fast sites, since the decay can be presumed to start at the end of the photolysis. However, if an appreciable fraction of the sites decay during the photolysis, which is certainly the case in our higher temperature traces, then the time $t = 0$ is not well defined. In addition, the absolute initial intensity (corresponding to an intact distribution) may not be known, which presents another problem. In order to use analytical functions to successfully fit our data, we would need to collect the decay traces in a manner which eliminates fast sites, i.e., one which allows observation of *all* the sites. The only way to accomplish this would be to decrease the photolysis time. However, preliminary modeling studies revealed that, at the higher temperatures, many sites would have very rapid decay rates, and no photolysis conditions could generate an adequate signal in a short enough time. Therefore, we abandoned this method of analysis.

The only decay-trace analysis method that we have used successfully is a simple numerical approach based on the forward Laplace transform.[12,14] The procedure calls for an initial assumption of distribution shape and then adjustment of parameters to produce the simulated decay trace that best fits the actual trace. Typically, distributions have two adjustable parameters, one relating to width and one relating to position on the rate axis.

This method has a disadvantage common with the above analytical methods, in that the distribution shape is chosen a priori. However, in the present case, we already know from the distribution-slicing experiments that the shape is Gaussian (or very nearly Gaussian), so the requirement of a shape assumption is no longer a disadvantage.

Studies using this basic method have been described in the literature,[12,14] though some of the previously used computational procedures diminish the flexibility of the method. These procedures fit the data in essentially the same manner as the analytical Laplace functions, thus introducing the same problem discussed earlier involving fast sites.

We recognized that this method had the potential for dealing with fast sites, so we developed a straightforward algorithm to accomplish this. The procedure involves computing the simulated decay trace point-by-point in a chronological sense. The distribution at each point is calculated from the distribution at the previous point, accounting for the decay occurring over the intervening time interval. The intensity at each point is simply the area under the current distribution. With this procedure, the photochemical-generation period can be included explicitly, accounting for both growth and decay during photolysis.

This approach correctly models the shapes of the decay traces we observe. However, as Figure 2b shows, the major feature that distinguishes different rates is the absolute intensity of the signal, rather than the shape. Thus, one needs a way to "normalize" the decay trace, i.e. to put it on an absolute intensity scale. The distribution-slicing data described above provide the necessary information. That is, any point in a distribution-slicing experiment corresponds to an *absolute* intensity for a given time at a given temperature. For example, Table I reveals that after 295 s at 34.3 K 53.5% of the sites will remain for **1**-Vin in MTHF. Thus, a decay trace determined at 34.3 K is normalized so that it crosses 53.5% at 295 s into the decay. Note that this procedure uses the raw time, temperature, and intensity data, so it does not introduce any assumption concerning log A or E_a.

The important point is that in exponential kinetics knowledge of initial intensity or even when the reaction started is unnecessary, since the $\ln f(t)$ versus t plot gives the same rate constant no matter when reaction monitoring is begun. However, *in nonexponenttal kinetics, knowledge of the absolute intensity is crucial, because*

(12) Siebrand, W.; Wildman, T. A. *Acc. Chem. Res.* **1986**, *19*, 238-243.
(13) Austin, R. H.; Beeson, K.; Eisenstein, L.; Frauenfelder, H.; Gunsalus, I. C.; Marshall, V. P. *Phys. Rev. Lett.* **1974**, *32*, 403-405.
(14) Jankowiak, R.; Richert, R.; Bässler, H. *J. Phys. Chem.* **1985**, *89*, 4569-4574. Albery, W. J.; Bartlett, P. N.; Wilde, C. P.; Darwent, J. R. *J. Am. Chem. Soc.* **1985**, *107*, 1854-1858. Richert, R. *J. Chem. Phys.* **1987**, *86*, 1743-1747. Plonka, A. *Time-Dependent Reactivity of Species in Condensed Media*; Springer-Verlag: Berlin, 1986. Hoffman, W. F., III; Shirk, J. S. *J. Mol. Struct.* **1987**, *157*, 275-287.
(15) Bellman, R.; Kalaba, R. E.; Lockett, J. A. *Numerical Inversion of the Laplace Transform*; American Elsevier: New York, 1966.
(16) Phillips, D. L. *J. Assoc. Comp. Machinery* **1962**, *9*, 84-97.

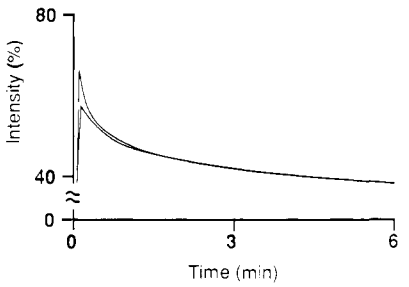

Figure 9. Simulated decay curves at 35 K, assuming log A = 8.0, E_a = 1.5 kcal/mol, and σ = 0.5 kcal/mol. The upper trace corresponds to no warming during photolysis, and the lower trace corresponds to a warming of 2 K.

this is the main feature that differentiates decay traces at various temperatures (see Figure 2).

We have incorporated our decay algorithm into two programs: a simulation program, DECAY, and a fitting program, FIT. DECAY serves two purposes: (1) simulated growth/decay traces are produced given log A, the most probable E_a, the choice of distribution shape and its width, and the temperature and (2) the E_a distribution at any point during the growth or decay can be displayed. (This program was used to produce the simulations in Figures 2 and 4.)

FIT produces growth/decay trace simulations in the same manner as DECAY, but the results are compared to an experimental trace (Figure 3). The distribution is handled on a logarithmic rate scale, which is proportional to E_a, so that log A input is not necessary. The distribution width and/or position on the axis can be optimized to produce the best fit.

At this point, the relationship between the E_a and rate axes should be clarified. The rate constant of the most probable site, $k°$, can be related to that of any other site in the distribution, k, by eq 7, where $\Delta E_a = E_a° - E_a$. Equation 7 shows that the ln

$$\ln (k/k°) = \Delta E_a/RT \quad (7)$$

$(k/k°)$ and ΔE_a scales are directly proportional. Further, whereas ΔE_a is temperature-independent, ln $(k/k°)$ varies inversely with temperature. The effect of this relationship is that an E_a distribution remains constant at all temperatures, while the corresponding ln $(k/k°)$ distribution becomes narrower as the temperature increases.

EPR-signal growth and decay curves were recorded for the cyclobutanediyls in the 4–55 K temperature range with photolysis intervals of 5–60 s. The signal decays, digitized and stored for later analysis, were followed for 12–25 min, even though at the lower temperatures only a small fraction of the signal decayed during this interval (see Figures 2b and 3). Monitoring signal decay over several half-lives, as is always desirable in quantitative kinetics, was impractical in our experiments. In most cases, this would have required experiments lasting days or weeks. Though experiments on the order of several hours may have been possible, these would not have resulted in significant improvement.

An experimental phenomenon which complicated the decay-trace analysis was a warming of the matrix caused by photolysis. This warming was detected and measured at 3.8 K through the Curie intensity effect (eq 8) and was found to be typically on the

$$\text{intensity} \propto 1/\text{temperature} \quad (8)$$

order of 1–3 K, with the matrix recooling immediately upon cessation of photolysis. Both the Curie effect and additional decay caused by the higher temperature are easily simulated using the algorithm of DECAY and FIT, and the result of such a warming (see Figure 9) is a flattening of the decay curve near the beginning. We therefore chose a point long after photolysis to normalize the decay traces.[17]

(17) The increases in temperature during photolysis obtained from the fitting procedures are often larger than 1–3 degrees (see Figure 3). This may be because the errors from other sources, such as temperature, width, and intensity normalization, are funneled into the heating optimization, since it is the last operation in the simulation.

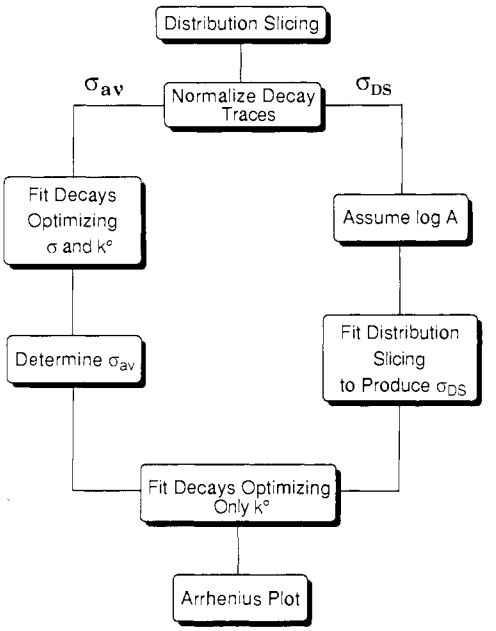

Figure 10. Flow chart depicting the two methods used to obtain activation parameters from experimental decay traces.

Table II. Most Probable Rate Constants for Cyclobutanediyls

biradical	solvent	T, K	$k°_{av}$, s^{-1}	$k°_{DS}$, s^{-1}
1-Vin	MTHF	20.2	1.45×10^{-12}	4.62×10^{-12}
		30.6	2.29×10^{-5}	2.73×10^{-5}
		34.5	9.85×10^{-4}	9.41×10^{-4}
		36.7	4.17×10^{-3}	3.76×10^{-3}
		39.8	2.36×10^{-2}	1.90×10^{-2}
		42.5	1.34×10^{-1}	1.00×10^{-1}
		44.9	2.46×10^{-1}	1.73×10^{-1}
		49.2	2.09	1.33
1-Vin	Heptane	27	7.27×10^{-5}	5.97×10^{-5}
		29	8.7×10^{-5}	7.4×10^{-5}
		32	2.73×10^{-3}	3.02×10^{-3}
		32	3.57×10^{-3}	4.07×10^{-3}
		35	2.00×10^{-2}	2.52×10^{-2}
		36	3.02×10^{-2}	3.98×10^{-2}
		38	1.36×10^{-1}	2.02×10^{-1}
		39	2.10×10^{-1}	3.22×10^{-1}
		46	3.39	6.37
		46	2.43	4.42
		54	4.62×10^{1}	1.04×10^{2}
1-EV	MTHF	20.5	4.4×10^{-7}	8.81×10^{-8}
		24	1.92×10^{-5}	9.00×10^{-6}
		26.6	1.95×10^{-4}	1.47×10^{-4}
		35.8	8.9×10^{-2}	2.00×10^{-1}
		41.0	6.58×10^{-1}	2.00
		44.1	1.33	7.00
1-Ph	MTHF	27	6.02×10^{-11}	
		34	1.86×10^{-7}	
		38.5	3.11×10^{-6}	
		43	1.94×10^{-4}	
		49.5	4.62×10^{-3}	
		54	4.08×10^{-2}	

Once the decay traces have been normalized with the distribution-slicing data, the fitting procedure is straightforward and can proceed in one of two manners. These are summarized in Figure 10. The first procedure, termed σ_{av}, uses the simulation package (FIT) to simultaneously optimize $k°$ and σ for each observed decay trace. This produces a different value of σ for each decay, but the observed variation is usually small. Since our model assumes that all initial distributions are the same, we average the various σ values to produce the one σ_{av} for a given biradical/solvent combination. We then refit the decays using σ_{av} and optimizing only $k°$. These $k°$ values (Table II) for the various temperatures are then plotted in an Arrhenius fashion to produce activation parameters. In the present case—**1**-Vin in MTHF—the value of σ_{av} is 0.554 kcal/mol, and an excellent Arrhenius plot is obtained

Table III. Activation Parameters for Cyclobutanediyls

		σ_{av}			DSFIT log A = 8		σ_{DS}	
biradical	solvent	σ_{av}	$E_a°$	log A	$E_a°$	σ_{DS}	$E_a°$	log A
1-Vin	MTHF	0.554	1.80	8.3	1.74	0.523	1.70	7.6
1-Vin	heptane	0.450	1.49	7.6	1.50	0.485	1.60	8.4
1-Vin	$CDCl_3$		*a*		1.25	0.420		*a*
1-EV	MTHF	0.432	1.16	6.0	1.44	0.533	1.40	7.8
1-EV	heptane		*a*		0.95	0.536		*a*
1-Ph	MTHF	0.600	2.29	7.8	2.34	0.488		*b*

[a] Decay traces not obtained. [b] Method gave unsatisfactory correlation with experimental data.

(Figure 11). The activation parameters are log A = 8.3 and $E_a°$ = 1.80 kcal/mol (Table III). We note that the kinetic point at 20.2 K was not included in the least-squares fit of the Arrhenius plot. The rate constant is very much smaller than the others (ca. 10^{-11} s^{-1}, Table III), and the extent of decay (Figure 3) is very small. As shown in Figure 11, though, the point is quite close to the line, a remarkable validation of the fitting scheme. Because of their presumed much larger error bars, we have not included such very slow rates (ln k < −20) in any of the Arrhenius fits.

The alternative approach, termed σ_{DS}, first assumes a value for log A (Figure 10). With this in hand, the distribution-slicing data can be fit by using DSFIT to produce a value for σ_{DS}. The rest of the procedure is then the same as for the σ_{av} approach (Figure 10). The choice of log A in the first step can be based on several types of evidence. One can use the log A determined from the σ_{av} approach (Table III). One can invoke experimental precedent, in that a variety of studies of spin-forbidden processes in hydrocarbons have been studied, as shown in Table IV. One can also estimate log A by what is, in effect, an iterative merger between the distribution-slicing and decay-trace data. For a given log A, each point on a decay trace can be related to a particular E_a value, according to eq 3. Then, after fitting the distribution-slicing data to a Gaussian by using DSFIT, the two data sets may be plotted on the same graph. As discussed in greater detail elsewhere,[7] the agreement obtained does depend on the choice of

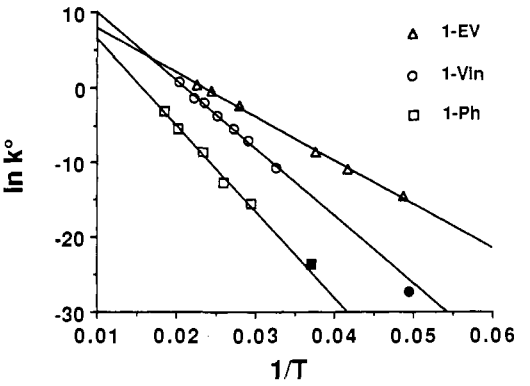

Figure 11. Arrhenius plots for **1**-Vin, **1**-EV, and **1**-Ph in MTHF. The rates were obtained by using the σ_{av} procedure. Data points corresponding to rate constants with ln $k°$ < −20 (filled markers) were not used in the least-squares analysis.

log A used in DSFIT. All three approaches indicate that spin-forbidden processes have low A values. We have chosen a log A of 8.0, which is consistent with precedent (Table IV) and with both the σ_{av} analysis (Table III) and the merged distribution-slicing and decay-trace analyses.

With a value of 8.0 for log A, DSFIT gives $E_a°$ = 1.74 kcal/mol and σ_{DS} = 0.523 kcal/mol (see Figure 8). The decay-trace fits using σ_{DS} are displayed in Figure 3 and produce the activation parameters log A = 7.6 and $E_a°$ = 1.70 kcal/mol, in excellent agreement with the distribution-slicing parameters (Table III). However, this agreement is somewhat artificial. When we repeated the decay trace fitting procedure with σ_{DS} values obtained with different log A values, the derived activation parameters more closely matched the new distribution-slicing parameters. Although the match cannot be taken as support for the absolute activation parameters, it does show that the results from the two experiments are consistent with each other, as they should be.

The two fitting schemes, σ_{av} and σ_{DS}, are in some senses complementary. An advantage of the σ_{av} approach is that *no as-*

Table IV. Activation Parameters for Triplet Biradical Reactions

reaction	log A, s^{-1}	E_a, kcal/mol	ref
	7.7–9.9	6–8	*a*
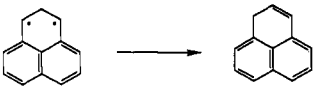	5.1 ± 1.0	5.3 ± 1.0	*b*
	8.4 ± 0.15	6.8 ± 0.2	*c*
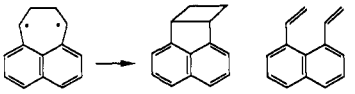	6.9 ± 0.3	4.5 ± 0.3	*d*
	10.4 ± 0.5	6.4 ± 0.3	*e*
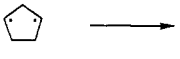	8.0	2.3	*f*
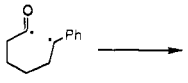	8.2 ± 0.1 7.7 ± 0.3	1.2 ± 0.1 0.8 ± 0.2	*g* *h*
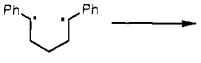	6.7 ± 0.2	0.85 ± 0.15	*i*

[a] Dowd, P.; Chow, M. *Tetrahedron* **1982**, *38*, 799–807. [b] Reference 10. [c] Hasler, E.; Gassman, E.; Wirz, J. *Helv. Chim. Acta* **1985**, *68*, 777–788. [d] Gisin, M.; Rommel, E.; Wirz, J.; Burnett, M. N.; Pagni, R. M. *J. Am. Chem. Soc.* **1979**, *101*, 2216–2218. [e] Platz, M. S. *J. Am. Chem. Soc.* **1980**, *102*, 1192–1194. [f] Reference 3. [g] Weir, D.; Scaiano, J. C. *Chem. Phys. Lett.* **1985**, *118*, 526–529. [h] Zimmt, M. B.; Doubleday, C., Jr.; Turro, N. J. *J. Am. Chem. Soc.* **1986**, *108*, 3618–3620. [i] Zimmt, M. B.; Doubleday, C., Jr.; Gould, I. R.; Turro, N. J. *J. Am. Chem. Soc.* **1985**, *107*, 6724–6726. [j] Products not determined.

sumption of log A is involved. The raw distribution-slicing data are used only to normalize the decay traces, and log A is obtained directly from the Arrhenius plot. A disadvantage to this approach is that it requires simultaneous optimization of two tightly coupled parameters (σ and $k°$) using curves that have a relatively low information content (Figure 3). The σ_{DS} procedure avoids this problem, but it requires an assumption of log A. This is perhaps not as severe a problem as it may seem, at least in the present case, since a variety of data suggests a value near eight. It is certainly reassuring that the two schemes produce such similar distribution widths and activation parameters (Table III).

It is worth emphasizing that *neither model assumed that the variation of k° with temperature would follow the Arrhenius law.* Yet, excellent correlations (Figure 11) are obtained over a very large temperature range (over a *factor* of 2) and a huge rate range (over 10 orders of magnitude). Given the difficulties of accurate temperature measurement and the complex analysis required to obtain $k°$, we consider these results to be quite compelling.

Results

1-Vin in MTHF. As described above, this structure produced σ_{av} = 0.554 kcal/mol, and the appropriate Arrhenius plot gave $E_a°$ = 1.80 kcal/mol and log A = 8.3 (Figure 11, Table III). With use of log A = 8.0, the fit of the distribution-slicing data gave σ_{DS} = 0.523 kcal/mol, which led to $E_a°$ = 1.74 kcal/mol (Figure 8). With this σ_{DS}, decay-trace fitting gave good fits to the kinetics data (Figure 3). An Arrhenius plot using these most probable rates ($k°$, Table II) gave an excellent linear fit with log A = 7.6 and $E_a°$ = 1.70 kcal/mol (Table III).

1-Vin in Heptane. The σ_{av} procedure gave σ_{av} = 0.450 kcal/mol, $E_a°$ = 1.49 kcal/mol and log A = 7.6 (Table III). Distribution-slicing data for **1**-Vin in heptane fit the Gaussian model quite well. Assuming log A = 8.0, the fitting procedure gave $E_a°$ = 1.50 kcal/mol and σ_{DS} = 0.485 kcal/mol. Decay-trace fitting using this σ_{DS} gave good fits and a quite satisfactory Arrhenius plot with $E_a°$ = 1.60 kcal/mol and log A = 8.4 (Table III).

1-Vin in $CDCl_3$. Only the distribution-slicing method was applied to **1**-Vin in $CDCl_3$. With an assumed log A of 8.0, a very good fit was obtained, with $E_a°$ = 1.25 kcal/mol and σ_{DS} = 0.420 kcal/mol (Table III).

1-EV in MTHF. All studies of **1**-EV indicated that it was less stable than **1**-Vin, which often made it more difficult to obtain strong signals. The σ_{av} procedure yielded σ_{av} = 0.432 kcal/mol, $E_a°$ = 1.16 kcal/mol, and log A = 6.0 (Table III, Figure 11). Distribution-slicing data were obtained and fit to a Gaussian assuming log A = 8.0. The fit, though worse than for **1**-Vin in MTHF, supported the qualitative observations in that $E_a°$ dropped to 1.44 kcal/mol with σ_{DS} = 0.533 kcal/mol. Decay-trace fitting with this σ_{DS} gave good fits to the decays, but the resulting Arrhenius plot showed considerably more scatter. The resulting activation parameters were log A = 7.8 and $E_a°$ = 1.40 kcal/mol (Table III).

1-EV in Heptane. Unfortunately, inefficient photochemical generation prevented the recording of decay traces for **1**-EV in heptane. However, several distribution-slicing experiments were performed. The results implied a much larger solvent effect than was observed for **1**-Vin. The curve for **1**-EV could not be fit with the assumption of an intact Gaussian distribution at 3.8 K, as was done for all the previous data. However, very good agreement was obtained by assuming 10% decay at the lowest temperature. The result, assuming log A = 8.0, is $E_a°$ = 0.95 kcal/mol and σ_{DS} = 0.536 kcal/mol (Table III).

1-Ph in MTHF. All studies of **1**-Ph indicate that it is the most persistent cyclobutanediyl of the series. For instance, **1**-Ph is indefinitely stable from 4 to 25 K, and an appreciable fraction of stable sites remains after warming to 65 K for 5 min. However, signals of **1**-Ph cannot be generated by prolonged photolysis at 77 K.[18]

Analysis of the data using the σ_{av} procedure gave σ_{av} = 0.600 kcal/mol. With this width to fit the experimental traces, activation parameters $E_a°$ = 2.29 kcal/mol and log A = 7.8 were obtained (Table III, Figure 11).

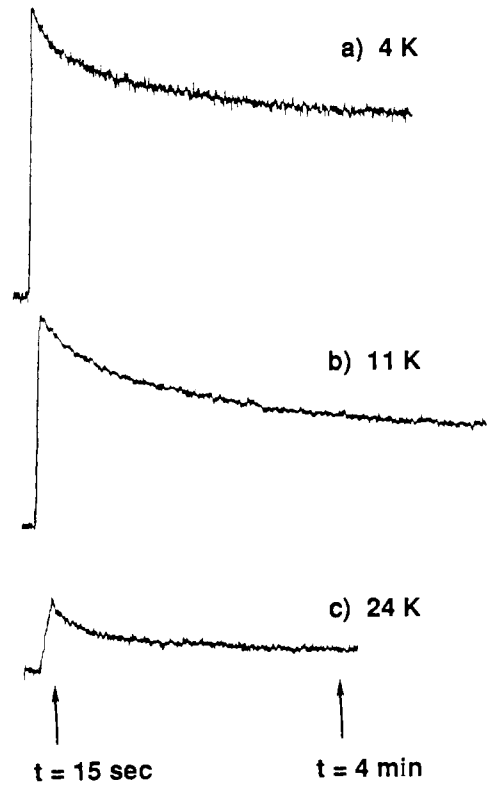

Figure 12. Decay curves for **1**-Et in MTHF.

A standard distribution-slicing experiment was also performed with log A = 8.0. Analysis of the data with DSFIT gave a satisfactory fit with σ_{DS} = 0.488 kcal/mol and $E_a°$ = 2.34 kcal/mol. However, when the decay traces were fit with this σ_{DS} value, noticeably poorer correlation with the data was observed. Also, although the most probable rates obtained produced satisfactory Arrhenius plots, a log A of 5.7 ($E_a°$ = 1.85 kcal/mol) was obtained, in poor agreement with the log A of 8.0 assumed for DSFIT. We thus believe that the results from σ_{av} are more reliable, and our discussion will emphasize them.

Fully Localized Biradicals 1-Me, 1-Et, and 3. The matrix-isolation decay behaviors of the fully localized biradicals **1**-Me, **1**-Et and Closs' biradical **3** are fundamentally different from those observed for the other structures discussed above. Even at 4 K, the EPR signal that is generated by photolysis decays significantly. Examples of such behavior for **1**-Et in MTHF are shown in Figure 12. Similar behavior was also seen for **1**-Me and **1**-Et in acetone and for **3** in cyclohexane. This instability at 4 K, of course, eliminates any possibility of a distribution-slicing experiment for these structures.

In analyzing the decay of **3**, Closs considered only initial decay rates[3] and found that they were relatively insensitive to temperature. From this it was proposed that quantum mechanical tunneling was involved in the decay of **3**, and indeed, a simple tunneling model fit the decay data well.

As described above, two characteristic features of composite first-order kinetics are a relative insensitivity to temperature and incomplete decay over a convenient time scale (see, for example, Figure 2). These characteristics are highly evident in Figure 12, and one might expect that the site distribution problem would be more severe at lower temperatures. We thus felt it was essential to investigate the possibility that the decays that we and Closs observed for the fully localized biradicals were in fact the result of a matrix-site effect operating on a low E_a process.

We have therefore applied our decay-trace fitting procedures to the fully localized biradicals. Since we have no distribution-slicing data, we used our fitting programs to simultaneously optimize three parameters: the distribution width, position, and

(18) Coms, F. D.; Dougherty, D. A. *Tetrahedron Lett.* **1988**, *29*, 3753-3756.

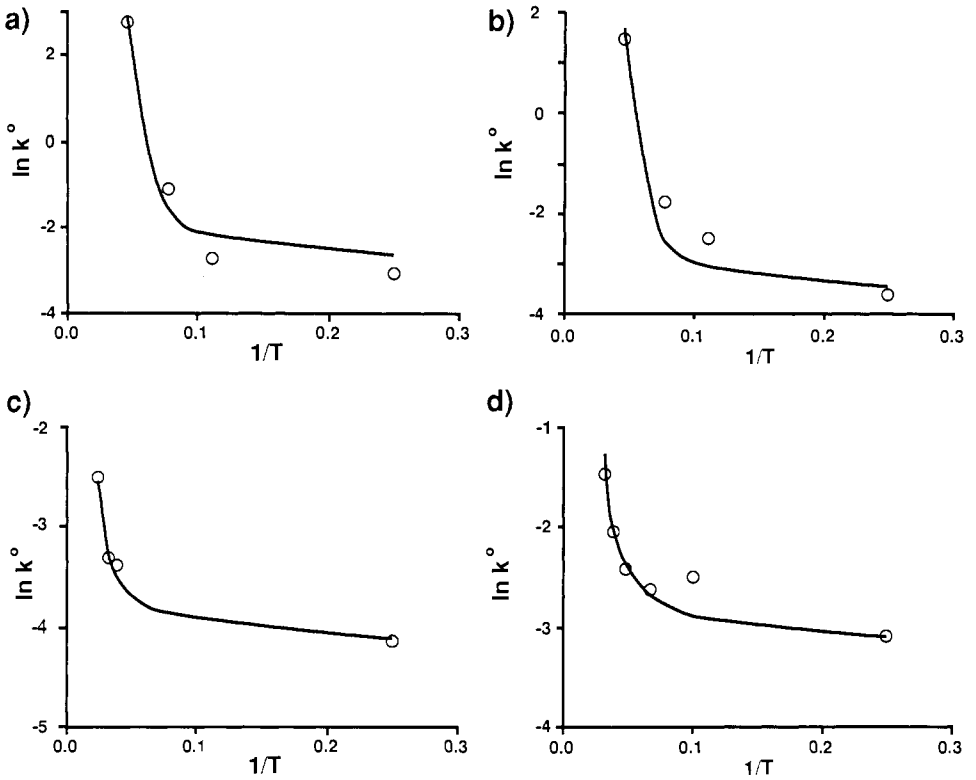

Figure 13. ln $k°$ vs $1/T$ data for (a) **1**-Me in acetone, (b) **1**-Et in acetone, (c) **3** in MTHF, and (d) **3** in cyclohexane. Points represent experimental data. Solid lines represent tunneling rates calculated with the parameters of Table VI.

Table V. Characteristic Parameters of Distributions Giving Best Fits to Decay Data for Fully Localized Biradicals

biradical	solvent	T,[a] K	$k°$	w[b]	σ, kcal/mol
1-Me	acetone	4	0.047	0.020	0.04
		9	0.068	0.016	0.10
		13	0.335	0.020	0.13
		22	15.9	0.033	0.18
1-Et	acetone	4	0.027	0.020	0.04
		9	0.081	0.020	0.09
		13	0.17	0.015	0.15
		22	4.37	0.033	0.17
3	cyclohexane	4	0.046	0.079	0.02
		10	0.083	0.065	0.055
		15	0.073	0.069	0.08
		21	0.089	0.060	0.12
		26	0.13	0.068	0.14
		32	0.23	0.079	0.16
3	MTHF	4	0.016	0.126	0.016
		26	0.034	0.093	0.12
		31	0.037	0.084	0.15
		42	0.082	0.097	0.19

[a] ±0.3 K. [b] See the text.

normalization. This procedure is, of course, intrinsically less precise and less accurate, and the results are compiled in Table V.

It is clear from the data of Table V, and from a variety of other fitting studies we have performed that *no* physically reasonable model based upon a distribution of sites with varying E_a values can mimic the decay behavior of **1**-Me, **1**-Et, and **3**. The temperature range involved in these studies is so immense (over a *factor* of 6 in some cases) that any feasible distribution that contains a significant number of intermediate and slow sites (Figure 4) at 4 K could not possibly have a significant number of intermediate and slow sites at 25 or 30 K.

The data of Table V show the remarkable insensitivity of $k°$ to temperature. For example, consider the data for **3** in MTHF. Assuming log A = 8.0, a $k°$ of 0.016 s^{-1} at 4 K implies $E_a°$ = 170 cal/mol. The predicted value of $k°$ at 42 K, then, is 4.1 × 10^6 s^{-1}, but the observed value is 0.082 s^{-1}.

Table VI. Tunneling Parameters[a]

structure	solvent	E_a, kcal/mol	$2a$, Å
1-Me	acetone	0.75	0.38
1-Et	acetone	0.825	0.325
3	MTHF	2.35	0.25
3	cyclohexane	1.60	0.29

[a] For all calculations $A = 10^8$ s^{-1} and the mass of the whole structure is used.

The simulations suggest another interesting result. If there were, in fact, a single, Gaussian distribution of E_a values, then for a given biradical/solvent combination all decay simulations should produce the same value for σ, the width of the Gaussian. Instead, we observed a clear trend toward increasing σ with increasing temperature (Table V). Interestingly, if one instead considers w, the width of the ln $(k/k°)$ distribution ($w = {}^1/_2(RT/\sigma)^2$), it is relatively constant, given the crude nature of the data (Table V). Such behavior is exactly what one would see if, instead of a distribution of E_a values, one had a single E_a value and a distribution of log A values. In order to reproduce the rates we observe, however, both log A and E_a have to be very small. For example, attempts to fit all or some subset of the data for **3** in MTHF always gave log $A < 0$.

All these observations suggest that quantum mechanical tunneling[19a] is involved in the decay of the fully localized biradicals.

(19) (a) Bell, R. P. *The Tunnel Effect in Chemistry*; Chapman and Hall: New York, 1980. (b) The rate expression must be modified to incorporate a tunneling correction factor Q. Thus,

$$k = QAe^{-E/RT}$$

where

$$Q = \frac{e^{\alpha}}{\beta - \alpha}(\beta e^{-\alpha} - \alpha e^{-\beta})$$

and

$$\alpha = \frac{E}{RT}$$

$$\beta = \frac{2\pi^2 a(2mE)^{1/2}}{h}$$

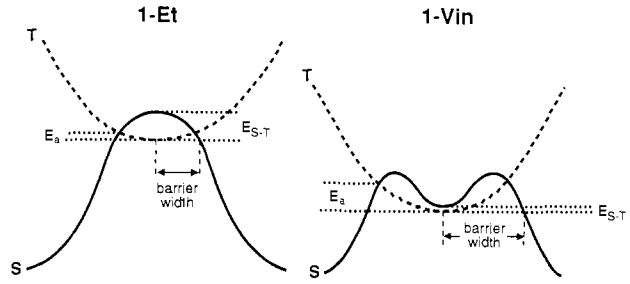

Figure 14. Schematic potential energy surfaces for the closure of cyclobutanediyls **1**-Et and **1**-Vin to the corresponding bicyclobutanes.

The relative insensitivity of $k°$ to temperature is, of course, the hallmark of a tunneling event. Also, to the extent that our simulations are meaningful, the relative constancy of the ln $(k/k°)$ distribution width (w) is also consistent with tunneling. That is, if one has a distribution of tunneling rates, as one would certainly expect, then not only should $k°$ be insensitive to temperature, but so should the relative rates of any two sites $(k/k°)$. Thus, the ln $(k/k°)$ distribution shape and width should not change dramatically with temperature.

Closs showed[3] that the rates he obtained for the decay of **3** could be readily modeled by using Bell's simple scheme[19] for tunneling through a parabolic barrier. The same is true for our data and, given the crude nature of the data, attempts to use a more sophisticated tunneling model are probably not justifiable. The results are summarized in Table VI and Figure 13. For the sake of consistency, all tunneling calculations assumed a log A of 8.0 and a mass (m) for the tunneling particle equal to the *entire mass of the biradical* (82 for **1**-Me, 110 for **1**-Et, and 68 for **3**). The choice of mass is somewhat arbitrary since, in the Bell model, m is tightly coupled to the barrier width $2a$. That is, the rate depends on $\sqrt{m}$ and linearly on $2a$. For example, if one would rather reduce m by a factor of 2, an identical simulation is obtained simply by increasing $2a$ by a factor of $\sqrt{2}$. Effectively, one can optimize only one member of the $m,2a$ pair (or in effect their product, $\sqrt{m}\cdot 2a$). We have used the extreme value for m simply to emphasize that significant tunneling rates through chemically meaningful barriers can be obtained even for very heavy particles.[20] In reality, it may be best to associate most of the mass with the radical carbons and their substituents, which presumably move the most in the ring closure (see below). Another difference between our analysis and Closs' is that we are reporting $k°$ values from our fitting procedure, rather than the initial rates.

With these assumptions, the fitting involves only two parameters. The first is barrier height, E, which determines the point at which the curve turns up, i.e., the onset of Arrhenius behavior. The second is the barrier width, $2a$. As shown in Figure 13, quite satisfactory fits can be obtained.

When tunneling is involved, isotope effects can be important. However, replacing the CH_3 groups of **1**-Me by CD_3[2a] does not produce a quantifiable change in decay behavior. Given the crude nature of the modeling for **1**-Me, small rate changes would not be observable. Our experimental observation of very little or no change upon deuteration is consistent with the notion that the reaction path involves motions by most or all of the atoms in the molecule. For example, using the parameters for **1**-Me from Table V1, but increasing the mass to 88, produces calculated rate changes of a factor of 2 at 10 K and less than 20% at 20 K.

Discussion

It is appropriate at this stage to consider the absolute accuracy of the parameters we have obtained. There is some uncertainty in the A values. For the best-behaved system, **1**-Vin, a large amount of data of several types strongly indicated that log A was in the range 7–9. We ultimately settled on a value of 8.0. This is certainly a reasonable value for a spin-forbidden process in a hydrocarbon, given the precedents of Table IV and a variety of laser-flash photolysis studies of triplet biradicals that indicate lifetimes of tens to hundreds of nanoseconds.[21]

Once a log A is obtained, the $E_a°$ values are really quite accurate. If one assumes that for a closely related series of molecules undergoing the same process all reactions should have the same A value, then the trends in $E_a°$ values are quite significant. A change in the assumed A would only shift the $E_a°$ scale. Similarly with the tunneling calculations, after assuming A, there are only two adjustable parameters: E determines the onset of Arrhenius behavior and $\sqrt{m}\cdot 2a$ sets the absolute rates. So, these parameters are fairly accurately determined, given a value for A.

It should be remembered that our model assumes that all matrix sites have identical A values. This is almost certainly untrue. However, attempts to simultaneously optimize A and E_a would introduce yet another adjustable parameter to a scheme that already involves fitting to curves with a fairly low information content. The distribution-slicing results require a variation in E_a, and as discussed above, relatively modest variations in E_a have much more profound consequences for the rates than do comparable variations in A, at cryogenic temperatures. Thus, we feel the assumption of constant A is the best course for this system.

We are now in a position to assess, to some extent, the influence of the matrix on the ring-closure reaction. It was clear from our initial spectroscopic studies that the matrix environment was not absolutely rigid. On the basis of analysis of EPR hyperfine splittings,[2] we were able to conclude that all cyclobutanediyls studied are planar or very nearly so. Since the four-membered ring is very highly puckered in the diazene precursor, considerable geometric relaxation must occur after N_2 loss. This relaxation is no doubt aided to some extent by the local heating that occurs on photolysis.

The very low temperatures involved in this work are certainly also a major reason that other distribution models were not applicable to our system. For example, the $t^{1/2}$ model implies a *rate* distribution that is not too dissimilar in shape from a Gaussian, but the width is much narrower than that required for the present systems. However, such a model is typically applied at $T \geq 77$ K, where an E_a distribution similar to the ones used here would produce a much narrower $k/k°$ distribution. For example, a 1 kcal/mol spread in E_a translates to a range of ln $(k/k°)$ values of 128 at 4 K but only 7 at 77 K. The $t^{1/2}$ model requires a temperature-independent full width at half maximum of ca. 2 ln $(k/k°)$ units. Many other studies have relied on initial rates, and again higher temperatures are often involved. In addition, the photolysis times are often quite long in such studies. Under these circumstances, one is sampling only the high E_a tail of the distribution, which could serve to attenuate matrix effects. It is clear from Figure 3, however, that under our conditions of short photolysis time and very low temperatures, the analysis of only initial rates would not be satisfactory.

A reasonable gauge of the magnitude of the matrix effect is the standard deviation of the Gaussian distribution, σ. There is a remarkable consistency of σ values, all falling in the range of 0.4–0.6 kcal/mol. It is actually a relatively small effect, of

(20) Carpenter, B. K. *J. Am. Chem. Soc.* **1983**, *105*, 1700–1701. Huang, M.-J.; Wolfsberg, M. *J. Am. Chem. Soc.* **1984**, *106*, 4039–4040. Dewar, M. J. S.; Merz, K. M., Jr.; Stewart, J. J. P. *J. Am. Chem. Soc.* **1984**, *106*, 4040–4041. Goldanskii, V. I.; Fleurov, V. N.; Trakhtenberg, L. I. *Sov. Sci. Rev., Sect. B* **1987**, *9*, 59–124.

(21) (a) Dervan, P. B.; Dougherty, D. A. In *Diradicals*; Borden, W. T., Ed.; Wiley: New York, 1982; pp 107–149. (b) Scaiano, J. C. *Acc. Chem. Res.* **1982**, *15*, 252–258. Caldwell, R. A.; Majima, T.; Pac, C. *J. Am. Chem. Soc.* **1982**, *104*, 629–630. Scaiano, J. C.; Wagner, P. J. *J. Am. Chem. Soc.* **1984**, *106*, 4626–4627. Johnston, L. J.; Scaiano, J. C.; Sheppard, J. W.; Bays, J. P. *Chem. Phys. Lett.* **1986**, *124*, 493–498. Akiyama, K.; Ikegami, Y.; Tero-Kubota, S. *J. Am. Chem. Soc.* **1987**, *109*, 2538–2539. Caldwell, R. A.; Sakuragi, H.; Majima, T. *J. Am. Chem. Soc.* **1984**, *106*, 2471–2473. Johnston, L. J.; Scaiano, J. C. *J. Am. Chem. Soc.* **1986**, *108*, 2349–2353. Closs, G. L.; Forbes, M. D. E. *J. Am. Chem. Soc.* **1987**, *109*, 6185–6187. Mizuno, K.; Ichinose, N.; Otsuji, Y.; Caldwell, R. A. *J. Am. Chem. Soc.* **1985**, *107*, 5797–5798. Sugawara, T.; Bethell, D.; Iwamura, H. *Tetrahedron Lett.* **1984**, *25*, 2375–2378. Burnett, M. N.; Boothe, R.; Clark, E.; Gisin, M.; Hassaneen, H. M.; Pagni, R. M.; Persy, G.; Smith, R. J.; Wirz, J. *J. Am. Chem. Soc.* **1988**, *110*, 2527–2538.

precisely the order of magnitude expected for noncovalent "lattice-packing" forces. The only reason we see such profound rate variations over different sites is the low E_a of the process we are investigating. Our simulations clearly show that if $E_a° = 25$ kcal/mol, then the decays seen (at temperatures around 300 K) for a Gaussian distribution with $\sigma = 0.5$ kcal/mol are not perceptibly different from those obtained with a single E_a.[22]

In many other studies of matrix-isolation decays, it is not difficult to imagine that in fact one is actually probing the nature of the matrix environment rather than the intrinsic reactivity of the species of interest. However, such studies almost invariably involve hydrogen abstraction from the matrix. Thus, the matrix material is one of the reactants in the system, so of course "matrix effects" are profoundly important. We feel there is good reason to believe that the *trends* we have observed in the present work are indicative of the intrinsic reactivities of the biradicals. The most compelling evidence in support of this is the fact that the steric interactions of a matrix with **1**-Et, **1**-EV, and **1**-Vin must be extremely similar, yet the three biradicals display qualitatively different behaviors. At present we cannot dissect the activation energies we obtain into a component due to matrix forces and a component that reflects the intrinsic reactivities of the biradicals. We think it is reasonable, though, to propose that the matrix effect is relatively constant for such closely related molecules, as evidenced by the invariance of σ (in the absence of tunneling). Thus, we feel that comparisons among the biradicals are chemically meaningful.

As mentioned previously, the molecules studied in the present work fall into two classes: stabilized and fully localized. The stabilized biradicals are persistent[23] at 4 K and undergo thermally activated decay at higher temperatures in accord with the Arrhenius law. Biradical **1**-EV, with only one stabilizing group, is less stable than those with two. Qualitatively, **1**-Ph is observable at significantly higher temperatures than **1**-Vin, and this is reflected in the larger $E_a°$ obtained for **1**-Ph.[24] The data set we have at present is limited, but the trend across the series of stabilized structures is satisfyingly consistent with one's chemical intuition.

Fully localized cyclobutanediyls decay via quantum mechanical tunneling. The process is qualitatively similar to that seen for cyclopentanediyl **3**, although the onset of Arrhenius behavior occurs at a lower temperature for the cyclobutanediyls. This factor is reflected in the smaller barrier heights E relative to **3** (Table VI). We have recently made a related observation, in that 1,3-diphenylcyclopentanediyl (**7**) is apparently much more stable than

7

1-Ph.[18] For instance, $k°$ for **7** at 77 K is ca. 10^{-4} s^{-1}, much less than what one would expect for **1**-Ph (see Table III). This suggests some generality for the greater stability of cyclopentanediyls vs cyclobutanediyls. This could be a manifestation of the reduced driving force for ring closure in the 5-membered ring system due to the greater strain increase in forming the ring-closed product. In addition, the larger separation between the radical centers in the 5-membered ring (2.37 vs 2.11 Å)[2,26,27] may require a much larger geometric distortion to achieve significant orbital overlap.

An important aspect of the cyclobutanediyl decays is that there are no H-shift (cyclobutene) products. In studies of **3** there are always small amounts of cyclopentene in the product mixtures. This left open the possibility that in fact the tunneling process was a hydrogen shift, a type of reaction for which tunneling is well precedented. The present studies greatly strengthen the conclusion that fully localized, triplet 1,3-biradicals can undergo C–C bond formation via tunneling. Tunneling also nicely explains our inability to observe the parent cyclobutanediyl, **1**-H. Apparently, the lighter mass of this species makes tunneling more efficient, and it decays too rapidly for EPR detection.[26] Simulating the decay of **1**-H with the above-described tunneling model supports this conclusion. In preliminary studies we have also been unable to observe 1-phenylcyclobutanediyl, suggesting that one unsubstituted carbon makes tunneling rapid. Heavy-atom tunneling has been the subject of several recent studies, and it may be quite common for highly reactive small molecules.[20]

One might ask why there is a qualitative difference in the decay behavior between the stabilized cyclobutanediyls and the fully localized ones. An interesting parallel exists in the cyclopropane thermal rearrangement literature.[21a,28] Theory suggests that the parent 1,3-biradical, trimethylene, should have no barrier to ring closure on the singlet surface, so it is not a true intermediate. Thermal rearrangement studies on cyclopropane-*1,2-d*$_2$ are consistent with this prediction, in that double methylene rotation is the dominant mode of stereomutation. In contrast, vinylcyclopropane, phenylcyclopropane, and other cyclopropanes with radical-stabilizing substituents display more conventional thermal behavior that is consistent with the intervention of a singlet 1,3-biradical as a true intermediate.

In light of these arguments, we can construct a model for cyclobutanediyl decay. Consider the contrasting behaviors of **1**-Et and **1**-Vin. We assume that delocalizing substituents preferentially stabilize the planar form of the biradical. This will introduce a well, or deepen a preexisting well, at the biradical geometry on the singlet (S) surface (Figure 14). In fact, in their classic analysis of biradicals, Salem and Rowland[29] proposed that the introduction of stabilizing substituents may be the only way to introduce a biradical minimum on the singlet surface. For the sake of argument, we shall assume that there is no singlet well for **1**-Et but that there is one for **1**-Vin. However, the analysis would be unchanged by the existence of a small barrier to closure for **1**-Et, as is suggested by recent theoretical work on the parent cyclobutanediyl.[26] We also assume that the S–T gap (E_{S-T}) in **1**-Vin is smaller than in **1**-Et. The T preference in these structures results from exchange repulsions, which depend upon the separation distance between the two radicals.[27a,29] Our spectroscopic studies[2] clearly show that delocalization keeps the spins further apart, which should diminish the exchange repulsions and the S–T gap in **1**-Vin.

The model is summarized in Figure 14. We assume that it is the spin forbiddeness of ring closure that is primarily responsible for the stability of the biradicals, and that intersystem crossing requires a near degeneracy of the S and T surfaces brought about by some geometric distortion. For **1**-Et, with no singlet biradical well, the transition state is approximated by the S–T crossing point.[26] Note that $E_a < E_{S-T}$ and that one has a small, narrow barrier. In **1**-Vin, both the S and T surfaces are stabilized by ca. 20 kcal/mol[25] relative to those of **1**-Et at biradical geometries. The introduction of a singlet well could move the surface crossing as shown to a point after the maximum on S. In this case, $E_a > E_{S-T}$ and the barrier width is substantially increased. In all tunneling models, the most important parameter is the barrier

(22) It has recently been demonstrated that at room temperature in fluid media there is a distribution of sites that show nonexponential decays on the femtosecond time scale. However, such fluctuations would be averaged out on the time scale of conventional kinetic studies. See, for example: Cruz, C. H. B.; Fork, R. L.; Knox, W. H.; Shank, C. V. *Chem. Phys. Lett.* **1986**, *132*, 341–344. Barbara, P. F.; Jarzeba, W. *Acc. Chem. Res.* **1988**, *21*, 195–199.

(23) Griller, D.; Ingold, K. U. *Acc. Chem. Res.* **1976**, *9*, 13–19.

(24) This stability ordering is the reverse of what one would expect on the basis of resonance-stabilization energies of allyl vs benzyl radicals (11.4 vs 10.1 kcal/mol).[25] The enhanced stability of **1**-Ph could arise from increased resistance offered by the matrix to structural reorganization involving motions of the much larger phenyl substituents, i.e., the phenyl groups are more tightly anchored in the matrix.

(25) Rossi, M.; Golden, D. M. *J. Am. Chem. Soc.* **1979**, *101*, 1230–1235.

(26) Pranata, J.; Dougherty, D. A. *J. Phys. Org. Chem.*, in press.

(27) (a) Goldberg, A. H.; Dougherty, D. A. *J. Am. Chem. Soc.* **1983**, *105*, 284–290. (b) Conrad, M. P.; Pitzer, R. M.; Schaefer, H. F., III *J. Am. Chem. Soc.* **1979**, *101*, 2245–2246.

(28) Berson, J. A.; Pedersen, L. D.; Carpenter, B. K. *J. Am. Chem. Soc.* **1976**, *98*, 122–143. Baldwin, J. E.; Barden, T. C. *J. Am. Chem. Soc.* **1984**, *106*, 5312–5319.

(29) Salem, L.; Rowland, C. *Angew. Chem., Int. Ed. Engl.* **1972**, *11*, 92–111.

width, $2a$, with the height, E, and mass, m, being less important. In our model for biradical decay, the width is essentially determined by how steeply the S surface falls. Introducing a well (or deepening an existing well) on S means that it initially rises and then falls, and this can increase the barrier width. Thus, **1**-Et and **1**-Me are presented with a fairly narrow barrier, through which tunneling is feasible, but **1**-Vin, **1**-EV, and **1**-Ph face too wide a barrier for tunneling. The model also nicely explains the increase in E_a on going from **1**-Et to **1**-Vin and why E for **1**-Et is smaller than 1.5 kcal/mol, the computed value of E_{S-T}.[26] Of course, at this point the model outlined in Figure 14 is strictly conjecture, and it will be interesting to see whether further examples support the basic scheme.

Conclusions

The cyclobutanediyls constitute a general class of triplet ground state, localized 1,3-biradicals. With stabilizing substituents such as vinyl or phenyl on the radical centers, the biradicals are indefinitely stable at 4 K. On warming to 20–50 K, ring closure commences, and the variation of the decay rates with temperature follows the Arrhenius law. The activation parameters are in accord with expectation, with log A in the 6–8 range and at E_a values of 1–2 kcal/mol.

In striking contrast, cyclobutanediyls that are devoid of stabilizing substituents decay even at 4 K. Reaction rates are remarkably insensitive to temperature, and quantum mechanical tunneling is involved in the ring closure. A model has been developed to rationalize the contrasting behaviors of stabilized vs fully localized cyclobutanediyls. Delocalizing substituents are thought to deepen the potential energy well in which the singlet biradical lies. This widens the barrier to ring closure and thus suppresses tunneling. The model rationalizes the observed trends in activation parameters and appears to be consistent with cyclopropane thermal rearrangement chemistry.

Analysis of the decay kinetics requires an explicit inclusion of matrix-site effects. This system can be quite well modeled with a Gaussian distribution of activation energies. The magnitude of the matrix effect—as estimated by the standard deviation of the Gaussian—is fairly small, on the order of 1 kcal/mol or less. However, at cryogenic temperatures such small perturbations can produce monumental rate effects. The key requirement for successful simulation is an absolute intensity measurement, i.e., a normalization of the decay curve. Given this, the methodology we have developed should be generally applicable to studies of dispersive kinetics.

Experimental Section

The synthesis of diazenes **2** and the EPR spectroscopy of biradicals **1** have been described in detail elsewhere.[2]

Distribution Slicing. The sample preparation and EPR instrumentation used have been described previously.[2] A strong triplet signal was generated by prolonged photolysis (20 s to 12 min) of the sample in the EPR cavity at 3.8 K. The intensity was recorded continuously throughout the experiment with occasional reference to an off-resonance base line. Care was taken to ensure that the signal was not saturated. At 3.8 K this was only possible for the $\Delta m_s = 2$ transition, typically at power settings of 0.02 mW or less. Warming of the matrix was accomplished either by restricting helium flow or by using the heater and automatic temperature control. In either case, equilibration was completed as quickly as possible without overshooting the desired temperature. Calibration of temperature was generally done before and after the experiment, the experimental temperatures being determined by interpolation of the available calibration points. The intensity after each cycle was measured following reequilibration to 3.8 K.

Decay-Trace Fitting. Decay traces were recorded by first equilibrating the sample in the EPR cavity to the desired temperature, which was determined by calibration immediately before and/or after the trace. With the spectrometer set to the field of the strongest transition, a signal was generated by photolysis through a combination of filters chosen to transmit a narrow band of radiation near 340 nm. Photolysis intervals were controlled by using a Vincent Associates Model SD-10 timed shutter and were kept only as long as necessary to generate an adequate signal. Base-line measurements at an off-resonance field were recorded before the generation and after the decay to allow later correction for any observed drift. The traces were digitized and stored on disk as collected with a Compaq Plus computer. Each data file contained 1000 intensity measurements. Decay traces were normally recorded at a nonsaturating microwave power, but higher power was sometimes used to allow shorter photolyses. No difference was distinguishable between saturated and nonsaturated traces, and the two types were fitted equally well in the analysis.

Acknowledgment. We thank the National Science Foundation for generous support of this work. F.D.C. was supported by a Jet Propulsion Laboratory/Center for Space Microelectronics Technology Fellowship sponsored by the Strategic Defense Initiative Organization/Innovative Science and Technology Office.

Registry No. **1**-H, 95580-29-3; **1**-Me, 92937-60-5; **1**-Et, 112422-81-8; **1**-Vin, 112422-86-3; **1**-Ph, 112422-85-2; **1**-EV, 112422-84-1.

Reactions of *N*-Halo-*N*-methylbenzylamines with MeONa–MeOH and *t*-BuOK–*t*-BuOH. Effects of β-Carbon Substituent and Base–Solvent System upon the Imine-Forming Transition State

Richard A. Bartsch*,[1a] and Bong Rae Cho*,[1b]

Contribution from the Department of Chemistry and Biochemistry, Texas Tech University, Lubbock, Texas 79409, and the Department of Chemistry, Korea University, Seoul, Korea.
Received August 1, 1988

Abstract: Elimination reactions of $YC_6H_4CH(R)N(X)CH_3$ in which R = Me and Ph and X = Cl and Br promoted by MeONa–MeOH and *t*-BuOK–*t*-BuOH have been studied kinetically. The elimination reactions are regiospecific, producing only the corresponding *N*-benzylidenemethylamines, and are quantitative when X = Cl. Comparison with published data for R = H reveals that with both base-solvent combinations variation of the β-carbon substituent from Me to H to Ph produces an increase in the ρ value, first an increase and then a decrease in k_H/k_D, and a decrease in k_{Br}/k_{Cl}. When the base–solvent system is changed from MeONa–MeOH to *t*-BuOK–*t*-BuOH, the ρ value increases, k_H/k_D remains nearly constant, and k_{Br}/k_{Cl} decreases for all three R groups. From these results, the changes in transition-state structure wrought by variation of the β-carbon substituent and the base–solvent system are assessed.

Extensive studies of olefin-forming, 1,2-elimination reactions have led to a detailed understanding of the relationship between E2 transition-state structure and changes in substrate structure, base–solvent combination, and other reaction variables.[2a,3] In

0002-7863/89/1511-2252$01.50/0 © 1989 American Chemical Society